JACS
JOURNAL OF THE AMERICAN CHEMICAL SOCIETY

ARTICLE

pubs.acs.org/JACS

Inhibition of Translation by Small RNA-Stabilized mRNA Structures in Human Cells

Kenichiro Ito,[†] Sou Go,[‡] Makoto Komiyama,[†] and Yan Xu*[,‡]

[†]Research Center for Advanced Science and Technology, The University of Tokyo, 4-6-1 Komaba, Meguro-ku, Tokyo 153-8904, Japan

[‡]Division of Chemistry, Department of Medical Sciences, Faculty of Medicine, University of Miyazaki, 5200 Kihara, Kiyotake, Miyazaki 889-1692, Japan

Supporting Information

ABSTRACT: RNA-mediated gene regulation and expression are critically dependent on both nucleic acid architecture and recognition. We present a novel mechanism for the regulation of gene expression through direct RNA−RNA interactions between small RNA and mRNA in human cells. Using mRNA reporters containing G-rich sequences in the 5′-untranslated region (5′-UTR), in the coding region, or both, we showed that G-rich small RNAs bind to the reporter mRNAs and form an intermolecular RNA G-quadruplex that can inhibit gene translation in living cells. Using a combination of circular dichroism (CD) and RNase footprinting in vitro, we found that the intermolecular G-quadruplexes show a parallel G-quadruplex structure. We next investigated whether the intermolecular G-quadruplex is present in living cells. Employing the fluorophore-labeled probes, we found that two G-rich RNA molecules form an intermolecular G-quadruplex structure in living cells. These results extend the concept of small RNA-mediated expression and suggest an important role for such RNA structures in the inhibition of mRNA translation.

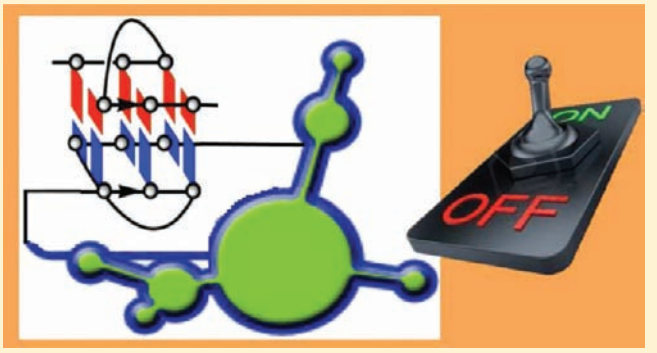

RNA molecules possess many important functions in the cell, which range from acting as a messenger to controlling the expression of various genes. RNA-mediated gene regulation and expression are critically dependent on both nucleic acid architecture and recognition and participation in base pairing and tertiary interactions.[1−3] miRNAs and siRNAs use base pairing to guide the interactions with their target mRNA.[4−7] A riboswitch is a part of an mRNA molecule that is known to undergo structural changes in response to the activity of a gene by binding a small target molecule.[8] Based on the known structural and functional diversity of RNA, it is not surprising that gene expression can be regulated by the conformational changes of an mRNA. In fact, a few examples have been reported wherein the formation of an intramolecular G-quadruplex (four-stranded RNA structure) within mRNAs has been proposed to be associated with cis-acting regulation.[9,10] Additional RNA-based mechanisms involve a variety of trans-acting RNAs that regulate gene expression by modulating the accessibility of the ribosome-binding site.[6,11] Here, we present a novel mechanism for post-transcriptional control of gene expression, which involves the formation of an intermolecular G-quadruplex between small RNA and mRNA. The RNA secondary structure-based regulation differs from that of the previously known small noncoding RNAs, which function by base pair-guided formation of double strands. In the novel mechanism, a four-stranded RNA structure is formed through a direct RNA−RNA dimerization interaction. This serves as a trans-acting function to extend the potential for small RNAs to regulate translation of a target mRNA sequence. In fact, we and others have shown by NMR and X-ray crystallography that human telomere RNA forms dimer G-quadruplex structures.[12−15] More recently, we found that human telomere RNA forms a G-quadruplex dimer in the living cells by employing a light-switching probe.[16]

RESULTS AND DISCUSSION

To investigate how small RNAs regulate translation through direct RNA−RNA interactions with mRNA in human cells, we constructed an enhanced green fluorescent protein (EGFP) reporter (EGFP1) containing a G-rich sequence in the 5′-UTR (Figure 1a and Supplementary Figure S1, Supporting Information). This sequence (5′-GGGCCCGGG-3′) is able to form an intermolecular G-quadruplex with a small RNA (ORN-1; G-rich sequence 5′-GGGUUAGGG-3′) (Figure 1a). Fluorescence imaging was used to monitor EGFP expression levels. Buffer treatment (without small RNA) enabled efficient expression of EGFP in the living cells to show that the mutated EGFP was properly expressed (Figure 1b). Transfection of cells with ORN-1 targeting the mRNA of EGFP was found to significantly

Received: July 8, 2011
Published: October 18, 2011

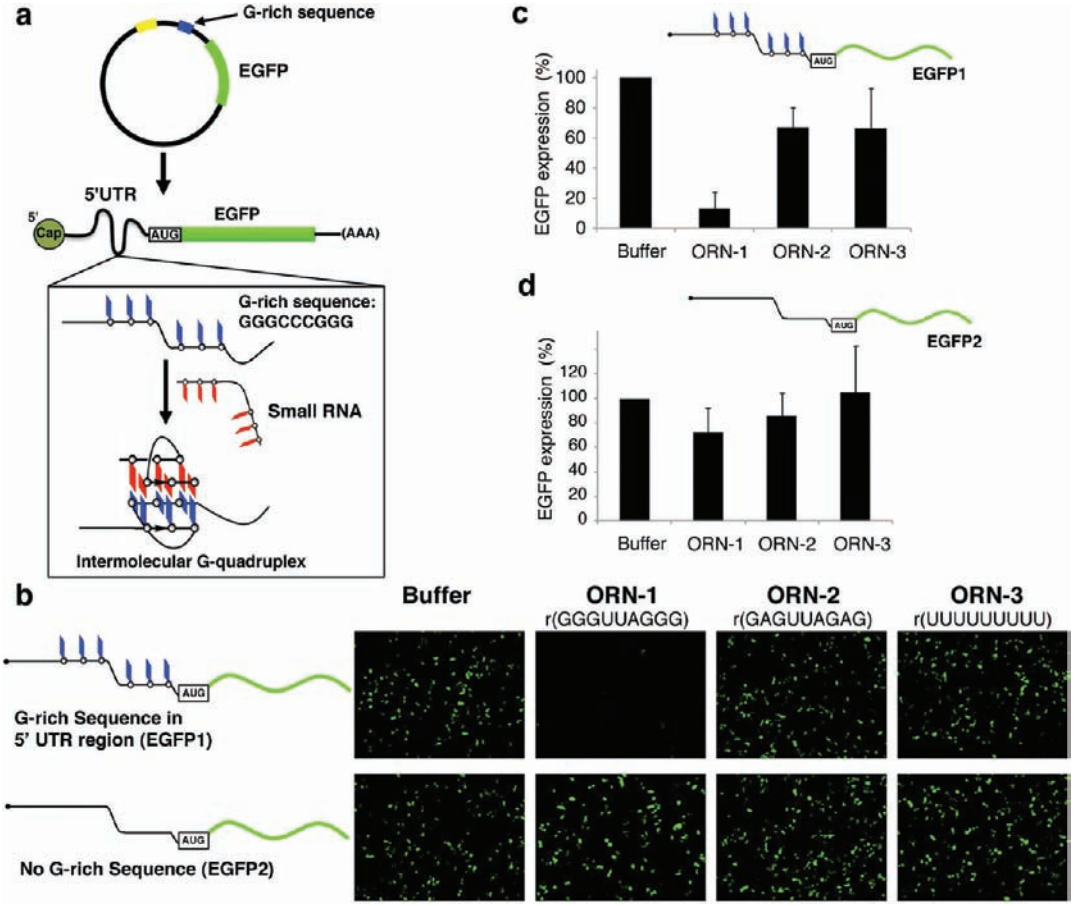

Figure 1. Translational inhibition through direct RNA—RNA interaction in the 5′-UTR. (a) Schematic representation of the mRNA of EGFP reporter constructs. The G-rich sequence 5′-GGGCCCGGG-3′ was incorporated into the 5′-UTR of mRNA. Small RNA has a G-rich sequence 5′-GGGUUAGGG-3′. The two G-rich sequences can form an intermolecular G-quadruplex. AUG indicates the start codon. (b) Fluorescence images showing small RNA effects in human cells. EGFP1, G-rich 5′-GGGCCCGGG-3′ sequence in the 5′-UTR region; EGFP2, no G-rich sequence; buffer, no RNA added; ORN-1, small RNA r(GGGUUAGGG); ORN-2, small RNA r(GAGUUAGAG); ORN-3, small RNA r(UUUUUUUUU). (c) Relative EGFP expression of EGFP1 treated with small RNAs and buffer and plotted as a percentage of the buffer-treated control, as evaluated by flow cytometry. Error bars represent SD. (d) Relative EGFP expression of EGFP2 treated with small RNAs and buffer and plotted as a percentage of the buffer-treated control. Error bars represent SD.

reduce EGFP expression relative to the buffer-treated cells (Figure 1b). Two mutated random-sequence RNAs (ORN-2, ORN-3) that did not contain the G-rich sequence were used in a parallel experiment. We found that these two RNAs were less efficient at interfering with EGFP expression (Figure 1b). Meanwhile, the other mRNA reporter (EGFP2), a negative control lacking the G-rich sequence, showed no repression of EGFP when combined with all the small RNAs (Figure 1b). To further clarify that the inhibition effect results from the G-quadruplex formation, we prepared a sequence ORN-1a (5′-UUUGGGCCC-3′) that would not favor G-quadruplex formation but it is Watson—Crick complementary to the target EGFP sequence ORN-5 (GGGCCCGGG) with 6 bases. We found that ORN-1a shows no repression of EGFP expression (Supplementary Figure S2, Supporting Information), suggesting G-quadruplex formation is the only way to inhibit EGFP expression.

To quantify the effects of the small RNAs, we employed flow cytometry to evaluate the level of EGFP expression. ORN-1 treatment of the cells resulted in an almost 7-fold decrease in EGFP with the G-rich reporter, whereas no significant repression was observed for ORN-2 and ORN-3 (Figure 1c and Supplementary Figure S3, Supporting Information). In addition, all small RNAs showed little effect on the control EGFP2 reporter, as expected (Figure 1d).

Encouraged by these data, we prepared two mRNAs (Figure 2a and Supplementary Figure S1, Supporting Information), one containing a G-rich sequence 5′-GGGCGAGGG-3′ in the coding region (EGFP3) and the other containing two G-rich sequences in the 5′-UTR and the coding region (EGFP4). This was done to test whether translation inhibition occurs in the other regions of mRNA. We designed two sequence changes in the coding region of the EGFP gene to obtain the G-rich sequence. Silent mutations in the coding region do not affect the encoded amino acid (Supplementary Figure S4, Supporting Information). Using the two reporters, we observed that the small RNA ORN-1 inhibits EGFP gene expression in human cells (Figure 2b—d and Supplementary Figure S3, Supporting Information). Although the reporter EGFP gene is known to be more strongly expressed in the mammalian cells, the intensity of EGFP expression was reduced to near background levels when the EGFP reporter was provided with two G-rich sequences (EGFP4) (Figure 2d).

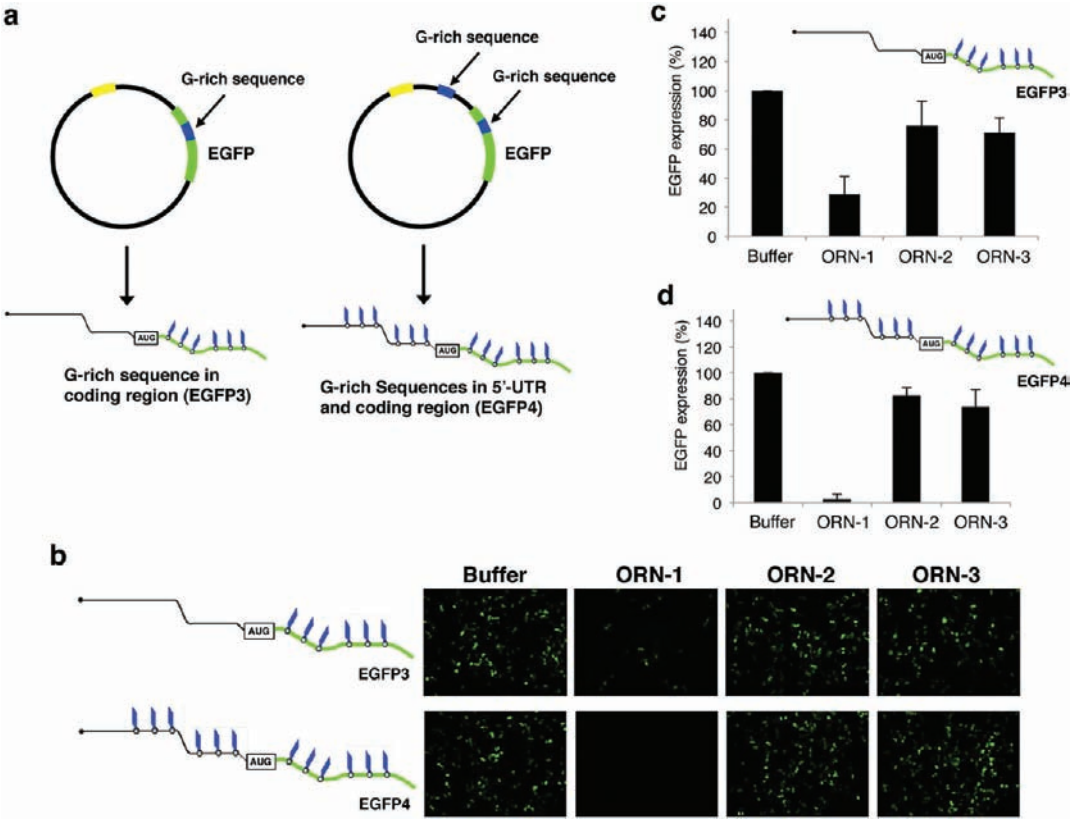

Figure 2. Translational inhibition through direct RNA−RNA interaction in the coding region. (a) Schematic representation of two EGFP reporter constructs. EGFP3, the G-rich sequence 5′-GGGCGAGGG-3′ was incorporated into the coding region of mRNA. EGFP4, the G-rich sequences 5′-GGGCCCGGG-3′ and 5′-GGGCGAGGG-3′ were incorporated into the 5′-UTR and the coding region, respectively. (b) Fluorescence images showing small RNA effects in human cells. EGFP3, the G-rich 5′-GGGCGAGGG-3′ sequence in the coding region; EGFP4, two G-rich sequences in the 5′-UTR and the coding region; (c) Relative EGFP expression of EGFP3 treated with small RNAs and buffer. Error bars represent SD. (d) Relative EGFP expression of EGFP4 treated with small RNAs and buffer.

To further characterize the inhibitory properties of small RNA, we examined the concentration-dependent effects of these RNAs on the inhibition of the EGFP targets. We found that the RNA-triggered inhibition of EGFP expression is dose dependent. Increasing amounts of ORN-1 (from 0 to 10 μM) effectively reduced the fluorescence intensity of EGFP (Figure 3a and Supplementary Figure S3, Supporting Information). Increasing the small RNA concentration to 2 μM leads to an almost complete inhibition of expression of EGFP4 (Figure 3a,b). We observed that the efficiency of inhibition of the EGFPs by the small RNA ORN 1 increases in the following order: EGFP3 < EGFP1 < EGFP4 (Figure 3b). This suggests that the suppression effect of small RNA in the 5′-UTR is stronger than that in the coding regions.

In order to further clarify that the inhibition effect results from the direct interaction of small RNA with mRNA and that it is not caused by altering the transcriptional efficiency of mRNA, we performed real-time PCR to measure the amount of EGFP mRNA. We found that for all small RNAs, the amount of mRNA barely decreased as indicated by the EGFP1−4 reporters (Supplementary Figure S5, Supporting Information). It is noted that putting the G elements into the coding region did not destabilize the mRNAs of reporters. The mRNA quantity of all reporters as shown in Figure S5, Supporting Information, strongly suggests that mRNA stability is not altered by the base changes. This indicates that small RNAs only affect translation and not transcription.

To prove that the interaction of small RNAs and mRNA is because of formation of an intermolecular G-quadruplex by the two RNA molecules, we first performed an experiment that included an RNA footprinting assay. The RNA footprinting assay has been used to identify the formation of the G-quadruplex.[17] Each G involved in the formation of a G-quadruplex is protected against RNase T1 (known as a strong RNase) degradation by the Hoogsteen bonds in the G-quadruplex. The cleavage pattern of G residues is used to probe the formation of the G-quadruplex. We prepared a FAM-labeled RNA (ORN-4) with G residues outside and inside the binding site. The G residues outside of the binding site should not be protected by ORN-1 binding, while G residues at the G-quadruplex site should be protected (Figure 4a). In the presence of ORN-2a, 5′-GAGGUGGAG-3′ (a mutated random-sequence control RNA having the same G bases with ORN-1), ORN-4, a fluorophore-labeled RNA containing the same G-rich sequence as in the 5′-UTR of EGFP1 (5′-GGGCCCGGG-3′) was randomly cleaved (Figure 4a, lane 3). However, in the presence of ORN-1 (a G-rich sequence), the G residues inside the binding site were found to be either partially or fully protected from cleavage whereas G residues outside the binding site were cleaved (Figure 4a, lane 4). Lane 1 of Figure 4a showed no cleavage in the absence of RNase T1. Lane 2 of Figure 4a, which lacked any RNAs but having T1, showed cleavage. Similarly, we observed the same cleavage pattern when using other labeled RNAs containing the same G-rich sequence

dx.doi.org/10.1021/ja206353c |J. Am. Chem. Soc. 2011, 133, 19153–19159

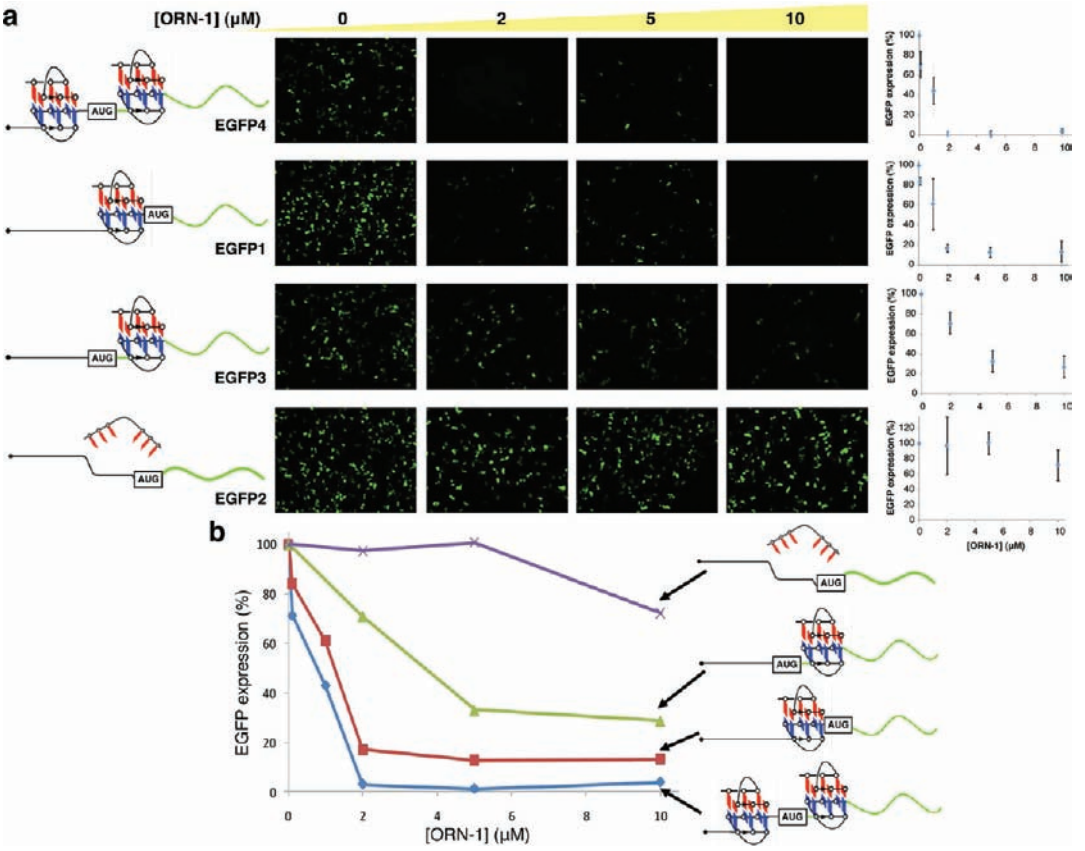

Figure 3. Concentration-dependent effects of small RNAs on inhibition of gene expression. (a) Fluorescence images showing the effects of small RNA in a concentration-dependent manner in human cells. The schematic representation indicates intermolecular G-quadruplex formation at different positions of the mRNA (EGFP1, EGFP3, and EGFP4) and non-G-quadruplex (EGFP2). Quantitation of EGFP expression plotted as a percentage of the buffer-treated control (right). Data are means ± SEM of three experiments. (b) Quantification of the expression of EGFP reporters treated with small RNA ORN-1.

as in the 5′-UTR of EGFP3 (5′-GGGCGAGGG-3′) (Supplementary Figure S6, Supporting Information). These results suggest that ORN-1 can form an intermolecular G-quadruplex with G-rich RNA.

To define the structural features of the intermolecular G-quadruplex, we examined the conformation of the complexes of ORN-1 and G-rich sequences (ORN-5 and ORN-6; G-rich sequences in the 5′-UTR and coding region) by circular dichroism (CD) spectroscopy. CD spectroscopy of the two complexes in the presence of K^+ showed a positive peak at 260 nm and a negative peak at 240 nm, which are the characteristic CD signatures of a parallel G-quadruplex structure (Figure 4b).[18−21] According to CD melting experiments, the T_m values of the two intermolecular G-quadruplexes in 200 mM KCl solution were ∼75 °C (Figure 4c). This demonstrates high thermodynamic stability. To further clarify that the inhibition effect results from the G-quadruplex formation, we investigated the thermal stability of ORN-1a (5′-UUUGGGCCC-3′) and target EGFP sequence ORN-5 (5′-GGGCCCGGG-3′). The melting experiments showed that ORN-1a/ORN-5 (T_m = 42 °C) (Supplementary Figure S7, Supporting Information) is significantly less stable than the ORN-1/ORN-5 ($T_m \approx 75$ °C).

We next prepared three RNA probes with fluorophores at their 3′-terminus to investigate whether an intermolecular G-quadruplex is present in living cells. For ORN-1-FAM and ORN-2-FAM probes, the FAM fluorophore is incorporated into the 3′-end of the G-rich sequence 5′-GGGUUAGGG-3′ (ORN-1) and the 3′-end of random-sequence 5′-5′-GAGUUAGAG-3′ (ORN-2), respectively. For the ORN-5-Cy3 probe, the Cy3 fluorophore is incorporated into the 3′-end of the G-rich sequence 5′-GGGCCCGGG-3′ (ORN-5). When two fluorophore-labeled probes are in the free form without G-quadruplex formation, both fluorophore molecules are spatially separated, and two colors can be observed. Formation of the G-quadruplex brings the fluorescent molecules at the 3′-ends into close proximity and produces a color change. We observed colocalization of the fluorescent signals (orange) when the Cy3-labeled probe ORN-5-Cy3 (red) and the FAM-labeled probe ORN-1-FAM (green) were transfected into living cells (Figure 5). This colocalization was not observed when the random probe ORN-2-FAM was used (Figure 5). These observations suggest that two G-rich RNA molecules form an intermolecular G-quadruplex structure; this is consistent with the recent results that a G-quadruplex dimer is formed in the living cells.[16] We further prepared two oligonucleotides having the light-switching pyrene probe at their 3′ and 5′ ends.[16] To document direct evidence for the presence of RNA G-quadruplexes in living cell, the oligonucleotides were applied to living cells (Supplementary Figure S8, Supporting Information). We observed excimer fluorescence of pyrene, whereas negative cells that were not treated with oligonucleotides remained virtually nonfluorescent. The results provide the in-cell evidence for the presence of the G-quadruplex.

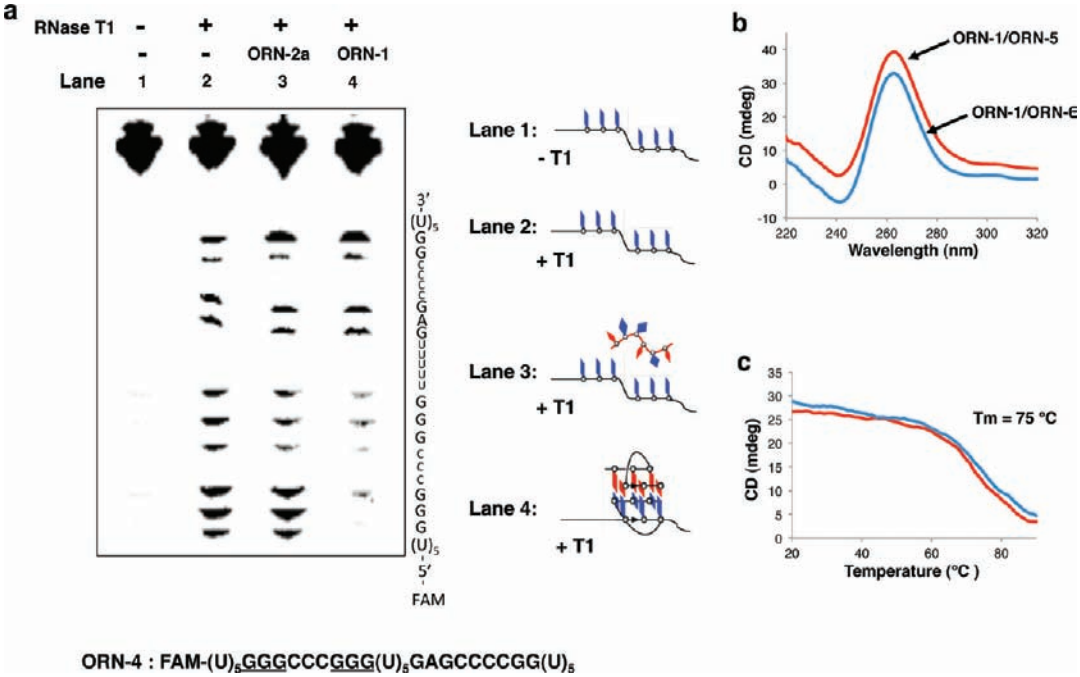

Figure 4. Intermolecular G-quadruplex formation by two RNA molecules. (a) RNase T1 footprinting assay for analysis of G-quadruplex formation. A representative gel electropherogram of a fluorescent FAM-labeled RNA (ORN-4, FAM-UUUUUGGGCCCGGGUUUUUGAGCCCCGGUUUUU) in the presence ORN-1 and ORN-2a or in the absence of RNase T1 is shown. Lane 1 shows RNA footprinting in the absence of RNase T1; lane 2 shows RNA footprinting in the absence of RNAs but having RNase T1; lane 3 shows RNA footprinting in the presence of ORN-2a (a mutated random sequence 5′-GAGGUGGAG-3′); lane 4 shows RNA footprinting in the presence of ORN-1 (G-rich sequence 5′-GGGUUAGGG-3′). (b) CD spectrometry for examining the structural features of the intermolecular G-quadruplex. ORN-1 is mixed with ORN-5 (5′-GGGCCCGGG-3′, G-rich sequence in the 5′-UTR) and ORN-6 (5′-GGGCGAGGG-3′, G-rich sequence in the coding region) in the presence of 200 mM KCl. (c) CD melting curves of ORN-1 with ORN-5 and ORN-6 monitored at 265 nm in the presence of 200 mM KCl.

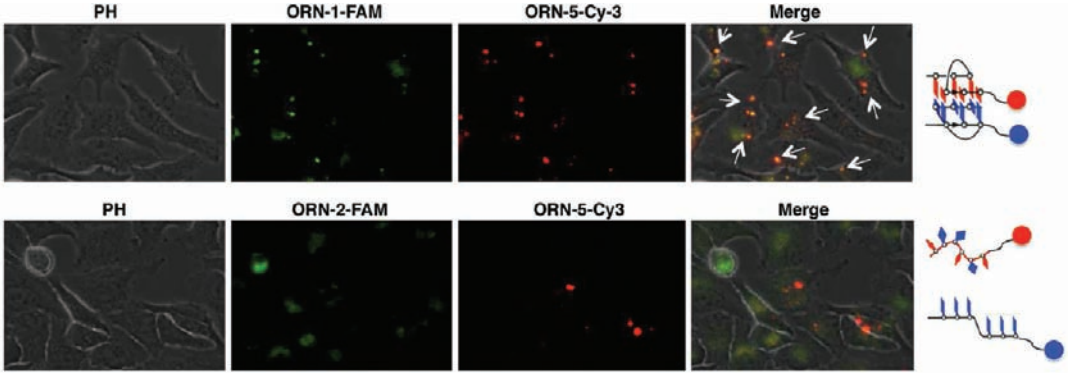

Figure 5. Fluorescence microscopy images of the intermolecular G-quadruplex in living cells. ORN-1-FAM, the FAM fluorophore is located at the 3′-end of the G-rich sequence 5′-GGGUUAGGG-3′ (ORN-1); ORN-2-FAM, the FAM fluorophore is located at the 3′-end of the random-sequence 5′-GAGUUAGAG-3′ (ORN-2); and ORN-5-Cy3, the Cy3 fluorophore is located at the 3′-end of the G-rich sequence 5′-GGGCCCGGG-3′ (ORN-5). ORN-1-FAM signals are in green, while ORN-5-Cy3 signals are in red. The colocalization of the two signals generates orange signals in the merged panel (arrows). For ORN-2-FAM and ORN-5-Cy3, there is no colocalization of fluorescent signals. PH indicates phase-contrast imaging.

In fact, intermolecular RNA interactions are critical for many biological processes. For example, RNA dimerization is a key step in the life cycle of retroviruses.[22] To date, RNA-mediated recognition is known to occur via base pairing in the mechanisms involving miRNA and siRNA. Our initial experiments suggest a new paradigm for the control of human gene expression involving tertiary interactions. Given that high-order structure guides these interactions with target mRNA, it is interesting that this observation has not been previously reported.

Although intramolecular RNA G-quadruplexes in the 5′-UTR appear to suppress gene expression, the translational regulation by formation of intermolecular G-quadruplexes may occur more widely in living cells.[23−26] One reason for this possibility is that the sequences that form intermolecular G-quadruplexes are much shorter than those forming an intramolecular G-quadruplex are. Such short sequences may be frequently present in mRNA. Another important point is that abundant noncoding small RNAs exist in the cells. For example, a noncoding RNA

molecule comprising telomeric repeat-containing RNA that includes mainly G-rich UUAGGG repeats of heterogeneous length has recently been identified in mammalian cells.[27,28] It is noted that 2 μM of the small RNAs used in the experiments is higher than the concentration of naturally occurring small RNAs. By use of the excess oligonucleotides, it is considered that RNase can degrade the small RNAs to decease their concentrations in cells. Large amounts of the small RNAs may be present in cells (although their concentrations may be lower than 2 μM), such as the recently discovered telomeric RNA.[27,28] Furthermore, some proteins have been suggested to be associated with G-quadruplex RNA, which may involve in the regulation of translation of lower concentration small RNAs.[29] On the basis of these findings and our study results, we reasoned that the interactions involved in the formation of the intermolecular RNA G-quadruplex may be frequently used to trigger recognition between two RNA molecules and regulate RNA translation.

METHODS

RNA Sequences and Plasmid Construction. The following RNA sequences were used in the study: ORN-1, 5′-GGGUUAGGG-3′; ORN-2, 5′-GAGUUAGAG-3′; ORN-3, 5′-UUUUUUUUU-3′; ORN-4, 5′-FAM-UUUUUGGGCCCGGGUUUUUGAGCCCCGGUUUUU-3′; ORN-5, 5′-GGGCCCGGG-3′; ORN-6, 5′-GGGCGAGGG-3′; ORN-7, 5′-FAM-UUUUUGGGCGAGGGUUUUUGAGCCCCGGUUUUU-3′; ORN-1a, 5′-UUUGGGCCC-3′; ORN-2a, 5′-GAGGUGGAG-3′; ORN-1-FAM, 5′-GGGUUAGGG-FAM-3′; ORN-2-FAM, 5′-GAGUUAGAG-FAM-3′; ORN-5-Cy3, 5′-GGGCCCGGG-Cy3-3′. pEGFP-N1 plasmid was purchased from Takara-Bio. Point mutations were inserted in pEGFP-N1 by PCR. The following DNA sequences were used as primers: EGFP1, 5′-CGGTACCGCGGGCCCGGGATCCACCGGTCG-3′ in 5′-UTR (forward); EGFP2, 5′-CGGTACCGCAGACCCAGAATCCACCGGTCG-3′ in 5′-UTR (forward) and 5′-CGTGTCCGGCGAAGGCGAAGGC-GATGCCAC-3′ (forward) in coding region; EGFP3, 5′-CGTGTCC-GGCGAGGGCGAGGGCGATGCCAC-3′ (forward) in coding region; EGFP4, 5′-CGGTACCGCGGGCCCGGGATCCACCGGTCG-3′ in 5′-UTR (forward) and 5′-CGTGTCCGGCGAGGGCGAGGGCGATG-CCAC-3′ (forward) in coding region. PCR was handled with Pfu Ultra (Stratagene) following the manufacturer's protocol. Products were treated with Dpn I, transformed to DH5α (TOYOBO). After culture, plasmids with point mutations were obtained using Plasmid Maxi Kit (QIAGEN). Sequences of reporters were determined by PRISM 3130 genetic analyzer (Applied Biosystems) according to the manufacturer's protocol.

EGPF Expression Studies and Microscope Assay. HeLa cells were grown at 37 °C and 5% CO_2 in Dulbecco's modified Eagle's medium (DMEM, 1.5 mL) containing 10% fetal bovine serum (FBS) and antibiotics (penicillin and streptomycin). Cells were seeded in a 96-well cell culture plate and incubated for 16 h. Plasmids (200 ng of each) were transfected to cells with 0.6 μL of FuGENE HD reagent (invitrogen). After transfection, 10 μM of each ORN (ORN-1, -2, -3) was added to medium. For various concentrations of transfection, 0−10 μM of ORN-1 was added. After 16 h of incubation at 37 °C, the cells were applied to various assays. An AF-6000 (Leica Microsystems) was used for observation of cells. The excitation and absorbance filter is 480/40 nm and 527/30 nm for detection of the fluorescence of EGFP and FAM and 546/12 nm and 600/40 nm for Cy3.

Flow Cytometry Analysis. Cells were counted with flow cytometry using Guava System (Millipore). Transfected cells were collected by tripsinization, washed in PBS, and resuspended in 300 μL of PBS. Only live cells were counted, and relative percentage of cells with fluorescent was calculated.

mRNA Quantification by Real-Time PCR. HeLa cells were seeded in 6-well cell culture plate and transfected with 2 μg of EGFP reporter. ORN-1 (40 μM) was added and incubated for 16 h at 37 °C. Cells were collected by tripsinization and washed with PBS buffer. mRNAs were isolated by 1 mL of ISOGEN, following the manufacturer's protocol and treated with RQ1 RNase-free DNase (Promega). mRNAs were reverse transcribed with Transcriptor High Fidelity cDNA synthesis kit (Roche). Samples were treated with RNase H (Takara). For real-time PCR reaction, Thunderbird qPCR mix (TOYOBO) was used. For internal standard, B2M gene was used as the housekeeping gene. Using CFX96 System (Bio-Rad), thermal cycle was carried out. To confirm singularity of product, melting curve analysis was used. The relative transcription efficiency of EGFP and B2M is calculated.

CD Measurements and CD Melting Analysis. CD spectra were measured using a Jasco model J-725 CD spectrophotometer with a 1 cm path-length cell. In CD melting studies, diluted samples were equilibrated at room temperature for several hours to obtain equilibrium spectra. The melting curves were obtained by monitoring a 260 nm CD band. ORN-1 (5 μM) with ORN-5 or ORN-6 were mixed in the annealing solution ([Hepes-HCl] = 5 mM, [KCl] = 200 mM, pH 7.0).

RNase T1 Footprinting. FAM-labeled RNAs (ORN-4, ORN-7; 2 μM) with 10 μM of ORN-1 or ORN-2a were mixed in the annealing solution. RNase T1 (0.02 U; Roche) was added to 10 μL of each sample and incubated at 37 °C for 1 min. Reaction was stopped by addition of 6 μL of urea loading buffer incubated at 95 °C for 2 min. Samples were analyzed by 20% denaturing PAGE, followed by visualization with GelStar (Lonza). FLA-3000 (FUJIFILM) and AE-9000-U (ATTO) were used for detection.

Fluorescent Analysis in Cells. FAM-labeled ORN-1 (40 μM; ORN-1-FAM) and ORN-2 (40 μM; ORN-2-FAM) were added to the medium with HeLa cells with 40 μM of ORN-5-Cy3. After 16 h of incubation at 37 °C and 5% CO_2, the cells were washed with HSBB once and fixed with 4% PFA in PBS for 15 min at rt. After being washed with PBS three times, the cells were analyzed by fluorescent microscopy.

ASSOCIATED CONTENT

Supporting Information. Supporting figures and chemical compound information. This material is available free of charge via the Internet at http://pubs.acs.org.

AUTHOR INFORMATION

Corresponding Author
xuyan@fc.miyazaki-u.ac.jp

ACKNOWLEDGMENT

This work was supported by a Grant-in-Aid for Scientific Research (B) from the Ministry of Education, Science, Sports, Culture, and Technology, Japan (No. 22350071).

REFERENCES

(1) Batey, R. T.; Rambo, R. P.; Doudna, J. A. *Angew. Chem., Int. Ed.* **1999**, *38*, 2326–2343.
(2) Hermann, T; Patel, D. J. *J. Mol. Biol.* **1999**, *294*, 829–849.
(3) Nowakowski, J.; Tinoco, I., Jr. RNA structure in solution. In *Oxford Handbook of Nucleic Acid Structure*; Neidle, S., Eds.; Oxford University Press: New York, 1999; pp 567−602.
(4) Filipowicz, W.; Bhattacharyya, S. N.; Sonenberg, N *Nat. Rev. Genet.* **2008**, *9*, 102–114.
(5) Bartel, D. P. *Cell* **2009**, *136*, 215–233.
(6) Storz, G.; Altuvia, S.; Wassarman, K. M. *Annu. Rev. Biochem.* **2005**, *74*, 199–217.

(7) Yue, X.; Schwartz, J. C.; Chu, Y.; Younger, S. T.; Gagnon, K. T.; Elbashir, S.; Janowski, B. A.; Corey, D. R. *Nat. Chem. Biol.* **2010**, *6*, 621–629.
(8) Mandal, M. *Nat. Rev. Mol. Cell Biol.* **2004**, *5*, 451–463.
(9) Kumari, S.; Bugaut, A.; Huppert, J. L.; Balasubramanian, S. *Nat. Chem. Biol.* **2007**, *3*, 218–221.
(10) Wieland, M.; Hartig, J. S. *Chem. Biol.* **2007**, *14*, 757–763.
(11) Majdalani, N.; Vanderpool, C. K.; Gottesman, S. *Crit. Rev. Biochem. Mol. Biol.* **2005**, *40*, 93–113.
(12) Xu, Y.; Kaminaga, K.; Komiyama, M. *J. Am. Chem. Soc.* **2008**, *130*, 11179–11184.
(13) Martadinata, H.; Phan, A. T. *J. Am. Chem. Soc.* **2009**, *131*, 2570–2578.
(14) Collie, G. W.; Haider, S. M.; Neidle, S.; Parkinson, G. N. *Nucleic Acids Res.* **2010**, *38*, 5569–5580.
(15) Xu, Y.; Ishizuka, T.; Kimura, T.; Komiyama, M. *J. Am. Chem. Soc.* **2010**, *132*, 7231–7233.
(16) Xu, Y.; Suzuki, Y.; Ito, K.; Komiyama, M. *Proc. Natl. Acad. Sci. U. S. A.* **2010**, *107*, 14579–14584.
(17) Darnell, J. C.; Jensen, K. B.; Jin, P.; Brown, V.; Warren, S. T.; Darnell, R. B. *Cell* **2001**, *107*, 489–499.
(18) Palumbo, S. L.; Ebbinghaus, S. W.; Hurley, L. H. *J. Am. Chem. Soc.* **2009**, *131*, 10878–10891.
(19) Xu, Y.; Noguchi, Y.; Sugiyama, H. *Bioorg. Med. Chem.* **2006**, *14*, 5584–5591.
(20) Datta, B.; Schmitt, C.; Armitage, B. A. *J. Am. Chem. Soc.* **2003**, *125*, 4111–4118.
(21) Xue, Y.; Kan, Z. Y.; Wang, Q.; Yao, Y.; Liu, J.; Hao, Y. H.; Tan, Z. *J. Am. Chem. Soc.* **2007**, *129*, 11185–11191.
(22) Badorrek, C. S.; Gherghe, C. M.; Weeks, K. M. *Proc. Natl. Acad. Sci. U. S. A.* **2006**, *103*, 13640–13645.
(23) Halder, K.; Wieland, M.; Hartig, J. S. *Nucleic Acids Res.* **2009**, *37*, 6811–6817.
(24) Huppert, J. L.; Bugaut, A.; Kumari, S.; Balasubramanian, S. *Nucleic Acids Res.* **2008**, *36*, 6260–6268.
(25) Arora, A.; Dutkiewicz, M.; Scaria, V.; Hariharan, M.; Maiti, S.; Kurreck, J. *RNA* **2008**, *14*, 1290–1296.
(26) Morris, M. J.; Negishi, Y.; Pazsint, C.; Schonhoft, J. D.; Basu, S. *J. Am. Chem. Soc.* **2010**, *132*, 17831–17839.
(27) Azzalin, C. M.; Reichenbach, P.; Khoriauli, L.; Giulotto, E.; Lingner, J. *Science* **2007**, *318*, 798–801.
(28) Schoefter, S.; Blasco, M. A. *Nat. Cell Biol.* **2008**, *10*, 228–236.
(29) Xu, Y. *Chem. Soc. Rev.* **2011**, *40*, 2719–2740.